ENTRAINMENT, DISPLACEMENT AND TRANSPORT OF TRACER GRAVELS

PETER R. WILCOCK

Department of Geography and Environmental Engineering, The Johns Hopkins University, Baltimore, Maryland 21218, USA

Received 18 April 1996; Revised 17 January 1997; Accepted 25 February 1997

ABSTRACT

The mass and size distribution of grain entrainment per unit bed area may be measured by replacing a volume of the bed with tracer gravels and observing the mass difference before and after a transport event. This measure of spatial entrainment is relevant to any process involving size-selective exchange of sediment between transport and bed and may be directly used in calculations of sediment transport rate using an elementary relation for fractional transport components presented here. This relation provides a basis for evaluating tracer data collected by different methods and may be used to provide physical insight regarding the expected behaviour of tracer grains. The variation with grain size of total displacement length L_{ti} depends on the degree of mobilization of the individual fractions on the bed surface: L_{ti} is independent of D_i for smaller, fully mobile sizes and decreases rapidly with D_i for larger fractions in a state of partial transport (in which a portion of the surface grains remain immobile through the flow event). The boundary between fully and partially mobile grain sizes increases with flow strength. These inferences are supported by values of L_{ti} calculated from flume experiments and provide a physical explanation for a summary relation between L_{ti} and D_i based on field data.

Earth surf. process. landforms, **22,** 1125–1138 (1997)
No. of figures: 4 No. of tables: 0 No. of refs: 26
KEY WORDS: bed-load transport; sediment transport; gravel-bed rivers; tracer techniques; field methods; sediment entrainment; grain displacement length.

INTRODUCTION

Sediment movement in gravel-bed rivers can be measured by direct sampling of the transport rate or by using tracer gravels to determine entrainment rates and grain displacement lengths. Although direct sampling is most common, tracer gravels offer some particular advantages and have found increased use in recent years (e.g. Emmett *et al.*, 1990; Church and Hassan, 1992; Hassan *et al.*, 1992; Schmidt and Ergenzinger, 1992; Haschenburger, 1996). Tracers are well suited to the stochastic and spatially variable nature of bedload transport because they are based on a predetermined bed sample composed of individual grains. For example, the entrained proportion of the bed surface and the size distribution of mobile and immobile grains may be measured with tracers, but not with direct sampling of sediment transport rate. Tracers also provide logistical and safety advantages because they may be installed during low flow, thereby avoiding direct sampling of bedload during floods.

The development of tagging methods that permit recovery of a large proportion of moved tracers (Ergenzinger and Conrady, 1982; Hassan *et al.*, 1984) has increased the accuracy of determining displacement distance and, therefore, transport rates from tracer observations. Tracers are likely to provide a more accurate measure of small transport rates, for which the errors associated with bedload samplers may exceed the measured rates. Where the accuracy of measuring transport rates with tracer gravels is comparable to that possible with direct sampling, the logistical advantage and additional information provided by tracer gravels make them an attractive alternative to direct sampling.

Contract grant sponsor: US Office of Naval Research; contract grant number: N00014-91-J-1192.
Contract grant sponsor: US National Science Foundation; contract grant numbers: EAR-9004206, EAR-9205511

CCC 0197-9337/97/121125–14 $17.50

This paper addresses several aspects of the collection, analysis and interpretation of tracer gravel observations, with the general objectives of increasing the information yield of a tracer gravel programme and improving the accuracy of transport estimates from tracer gravels. First, a method is described for using tracer gravels to accurately measure the total mass and the size distribution of sediment entrained per unit bed area. Direct measurements of these quantities are immediately relevant to mechanisms of sediment exchange between the transport, bed surface and bed subsurface, and supplement work on the vertical mixing of tracer grains (e.g. Schick *et al*., 1987; Hassan and Church, 1994). The accuracy of bedload calculations depends equally on the quality of entrainment and displacement observations, so the method presented here complements the recent advances in tracer recovery and displacement estimates. In practice, tracer measurement of sediment entrained per unit bed area provides a useful complement to scour chains and other scour depth indicators and should give a superior measurement of entrainment at small transport rates with negligible bed scour.

The second objective of the paper is to present an elementary relation between transport rate, displacement length, and the spatial entrainment of different grain sizes. An explicit statement of the relation between transport rate and its components is needed not only to calculate transport rate, but also to compare different types of tracer measurements, and to evaluate tracer observations from different flows and locations. The transport component relation distinguishes between terms that have time-invariant average or limiting values and terms that vary directly with the duration and rate of transport. The former are suitable for direct comparisons among different flow strengths and sediments; unless suitably scaled, comparison of the latter results from stream to stream is not particularly meaningful, because they become arbitrarily large or small depending on the transport duration.

The final objective of the paper is to use the explicit relation for transport components to illustrate the functional dependence of the individual components, thereby providing a physical basis for evaluating field observations. The expected variation with grain size of tracer displacement length is developed and illustrated using displacement lengths calculated from measurements of entrainment, surface size distribution and transport rate in laboratory experiments. These results are compared to a summary relation for displacement lengths observed in the field (Church and Hassan, 1992), leading to a suggested physical mechanism for the observed relation.

ENTRAINMENT FROM LARGE TRACER GRAVEL INSTALLATIONS

If all grains in an area of the bed are replaced by tracer gravels to a depth greater than the scour depth, comparison of the mass of tracers before and after a flow event provides a direct measure of the sediment entrainment per unit bed area M_a. The product of M_a and the total displacement length of mobilized tracers is the mean bed material transport rate. Such a tracer gravel installation also provides a local measure of the proportion of the bed surface mobilized and the size distribution of mobilized grains.

For installation, the tracer gravel method presented here consists of little more than marking and replacing all the grains that would be collected in a large sample of the bed material size distribution. A large metal cylinder (e.g. a cut-off oil drum) is worked into the bed as deeply as possible (similar to the method of McNeil and Ahnell (1964) but with a larger sampler). Use of a cylinder provides a well-defined sample volume and permits both subaerial and underwater sampling, as long as the water depth is shallow enough to permit access to the cylinder interior (roughly less than 0·5 m). All sediment down to the bottom of the sampler may be removed manually or by using a freeze-core device within the cylinder (Rood and Church, 1994). The size of cylinder should be selected to provide a sample of sufficient size to give an accurate measure of the bed size distribution. We have used cylinders of 60 m diameter and recovered samples as large as 280 kg by removing sediment to a depth of 45 cm. The depth of the sample is measured by surveying the bed before and after removing the sample.

After the size distribution of the sampled sediment is determined, the sediment is painted and returned to the sampler and the cylinder is removed from the bed. Complete recovery of all immobile tracers can be facilitated if only a portion of the bed sample is marked and returned to the centre of the sample volume using a smaller cylinder placed within the first cylinder. The disturbance produced by removing and replacing sediment may be partly mitigated by dividing the sample into vertical subsamples which are then returned to the bed in reverse

order. Accurate vertical subsamples may be manually collected for the subaerial case. For samples in the wetted portion of the streambed, vertical segregation of the fine fractions is difficult to maintain with manual sampling and the combined cylinder–freeze-core technique of Rood and Church (1994) is a useful alternative.

This tracer method requires considerable labour. For gravel and cobble beds, the size of a representative sample can be several hundred kilograms (Church *et al*., 1987; Rood and Church, 1994). We find that one or two samples can be installed in a day by a team of two people (Wilcock *et al*., 1996). The fieldwork may be expedited if premarked tracer grains are used, thereby saving the time required to dry and paint the sample. In this case, the native gravel is replaced by marked grains matching the number and shape of grains of each size. Grains larger than 8 to 16 mm may be replaced by the number and shape of grains in each size class. Sand and granule sizes are conveniently replaced on a total mass basis using brightly painted sediment such as may be found commercially for aquarium use. The effort involved in installing large tracer gravel samples is balanced by the fact that such samples are necessary to determine the size distribution of the bed so that, in many cases, much of the sampling effort may already be part of the field programme.

After the flow event, the tracers are resampled to determine the mass of grains of each size remaining in place, from which the total entrained mass M_e and the entrained mass of each size M_i may be calculated. Dividing by the sample area gives the mass entrainment per area on a total (M_a) or size-fraction (M_{ai}) basis. The total depth of bed scour, or exchange depth d_x, is calculated as $d_x = (M_e/M_t)d_s$, where M_t is the initial mass of tracer grains, (M_e/M_t) is the proportion of entrained grains, and d_s is the surveyed sample depth. A fractional exchange depth d_{xi} may be calculated as the entrained proportion of grains of each size multiplied by the sample depth. To provide a consistent comparison among samples with different grain size and sample depth, the exchange depth may be scaled by the thickness of the bed surface layer, for which D_{90} provides an appropriate estimate. The scaled exchange depth is:

$$\frac{d_x}{D_{90}} = \frac{M_e}{M_t}\frac{d_s}{D_{90}} \tag{1}$$

Because $M_t(D_{90}/d_s)$ approximates the mass of grains in the surface layer, d_x/D_{90} may be interpreted as the exchange depth expressed in multiples of the surface layer thickness. For $d_x < D_{90}$, Equation 1 provides an estimate of the mobilized proportion of the bed surface. A similar interpretation can be given to the scaled fractional exchange depth d_{xi}/D_{90}. Values of $d_{xi}/D_{90} < 1$ indicate a state of partial transport, in which only a portion of the surface grains of a given size are mobilized over the duration of the transport event (Wilcock and McArdell, 1997).

An example of the information provided by large tracer gravel installations is given in Figure 1, in which the scaled fractional exchange depth d_{xi}/D_{90} is plotted as a function of total exchange depth d_x/D_{90} for two reaches on the Trinity River, California (Wilcock *et al*., 1996). The data plotted represent the mean of three samples at each of three locations for two reservoir releases of different magnitude. Two groups of samples were collected in both reaches at the lower flow, and one group of samples in both reaches at the higher flow. The samples were collected manually in a water depth of 0·5 m or less.

The fractional exchange depths broadly follow the total exchange depth, although with some size-dependent variation. For very little entrainment ($d_x/D_{90} \leq 0{\cdot}1$), the finest sizes at both sites show weak partial transport ($0{\cdot}2 < d_{xi}/D_{90} < 0{\cdot}4$), whereas all coarser sizes are essentially immobile. For $d_x/D_{90} \approx 0{\cdot}4$ and all sizes finer than D_{98}, some grains of each size are moved although all sizes are in a state of partial transport ($d_{xi}/D_{90} < 1$), with the exception of D_{66} at Poker Bar, an outlier that appears not to be representative of the local entrainment. For complete surface entrainment ($d_x/D_{90} \approx 1$) at the Steelbridge site, sizes larger than 90 mm ($\approx D_{72}$) are in a state of partial transport, whereas $d_{xi}/D_{90} \geq 1$ for all finer sizes. For $d_x/D_{90} \approx 1{\cdot}4$ at the Poker Bar site, the surface portion of sizes larger than 32 mm ($\approx D_{60}$) is completely mobilized ($d_{xi}/D_{90} \approx 1$), whereas the finest two fractions have $d_{xi}/D_{90} > 1{\cdot}8$. For d_x larger than 10 or 20 per cent of D_{90} grains of all sizes are entrained and fractional exchange depths fall within a factor of two, with the very largest fractions tending to have the smallest entrainment.

Comparison of the entrainment with local flow observations (Wilcock *et al*., 1996) shows that the threshold between negligible grain movement and entrainment of most of the bed surface occurs over a narrow range of local bed shear stress τ_0 on the order of 10–15 per cent. A scour depth equal to the thickness of the bed surface

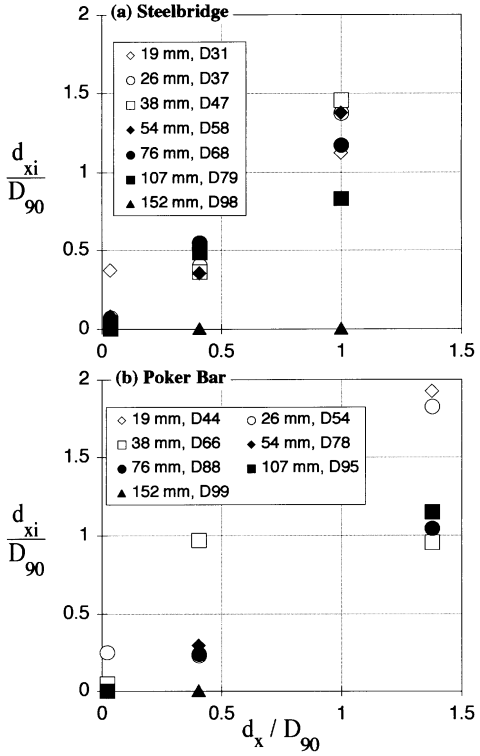

Figure 1. Fractional exchange depth as a function of total exchange depth for large tracer gravel installations on the Trinity River, California: (a) Steelbridge reach; (b) Poker Bar reach. The symbols at each value of d_x/D_{90} represent the mean of three tracer samples. Samples with $d_x/D_{90}<0{\cdot}5$ are for a release of $Q=76\,m^3\,s^{-1}$; for $d_x/D_{90}\geq1{\cdot}0$, $Q=164\,m^3\,s^{-1}$. Mean channel width is 35 m. Fractional exchange depth scales with total exchange depth, although d_x/D_{90} values for the finest fractions tend to be somewhat larger and d_x/D_{90} values for the coarsest fractions are smaller. Under conditions of partial surface mobilization ($d_x/D_{90}<1$), grains of all sizes are entrained (except the very largest, D_{98}) and are in a state of partial transport

layer occurs at $\tau^*_g\approx0{\cdot}035$, where τ^*_g is the dimensionless shear stress $\tau_0[(s-1)\rho g D_g]^{-1}$, $s=\rho_s/\rho$, ρ_s and ρ are sediment and fluid density, g is the acceleration of gravity, and D_g is the median grain size of the gravel portion of the bed size distribution. Both entrainment and transport rates decrease rapidly with smaller τ^*_g, with the bed becoming nearly immobile at $\tau^*_g\approx0{\cdot}031$. These values of τ^*_g are within the range for the critical shear stress of gravel in well-controlled laboratory experiments, demonstrating that local observations of flow and entrainment may be made with similar accuracy in the field (Wilcock *et al*., 1996).

TRANSPORT COMPONENTS

Calculations of transport rates from tracer observations, as well as comparisons between different tracer measurements, require a formal statement of the relation between transport rate, entrainment and displacement. To facilitate comparison between different sediments and flows, it is useful to express the individual transport components in a form that may be expected to have a time-invariant mean under steady-state transport conditions. An appropriate form is:

$$\bar{q}_{bi} = M_{ai}\left(\frac{N_i}{T}\right)L_{1i} \tag{2}$$

where the equation is in units of $[ML^{-1}T^{-1}]$, M_{ai} is the mass of fraction i entrained per unit bed area over the time period T, N_i is the number of times an individual grain of fraction i is entrained during T, and L_{1i} is the length of a

single displacement. M_{ai} represents the entrainment of the sediment found in a given bed area at the start of T, as would be measured by tracer gravels.

Although each transport component may be represented by a frequency distribution (e.g. Einstein, 1937; Stelczer, 1981; Kirkby, 1991; Hassan *et al*., 1991), the focus here is their mean values, as defined in Equation 2. The product of means in Equation 2 is equivalent to the ensemble average product for some plausible frequency distributions of the transport components (e.g. an exponential or gamma distribution for L_{1i}, as suggested by Einstein (1937), and recently evaluated using tracer gravels by Hassan and Church (1992) and Schmidt and Ergenzinger (1992)). For other possible frequency distributions, the terms in Equation 2 must be regarded as 'effective' averages, in the sense that they are defined such that their product gives the mean q_{bi}.

Under steady-state transport conditions, q_{bi} varies about a constant mean. M_{ai} may be expected to approach a nearly constant value as the entrainable grains are removed from an area of the bed. Note that this does not mean that entrainment ceases, but that an increasing proportion of the entrainment is composed of grains originating from a different area of the bed. Wilcock and McArdell (1997) found that, under constant flow conditions, M_{ai} approaches a nearly constant value once the cumulative transport exceeds roughly twice the mass of the actively transported bed surface layer. If it is assumed that the mean value of L_{1i} does not vary under steady-state transport conditions, it follows from Equation 2 that (N_i/T) must also have a constant mean value, leading to the plausible assumption that N_i increases directly with time.

In some cases, the basic measured quantity is a combination of the transport components in Equation 2. The rate of entrainment of grains found within a specified unit bed area is given by M_{ai}/T and the instantaneous rate of entrainment per unit bed area (regardless of grain provenance) is given by $M_{ai}N_i/T$. The latter quantity has been measured on films of bedload transport by counting all entrainments from a fixed area over a measured duration (Fernandez Luque and Van Beek, 1976; Drake *et al*., 1988). The two quantities most commonly observed with tracer gravels are the total displacement length $L_{ti} = N_i L_{1i}$ and the virtual grain velocity $u_{vi} = (N_i L_{1i})/T$. If q_{bi} and M_{ai} are measured, L_{ti} and u_{vi} may be calculated from Equation 2 as:

$$L_{ti} = \frac{q_{bi} T}{M_{ai}} \tag{3}$$

and

$$u_{vi} = \frac{q_{bi}}{M_{ai}} \tag{4}$$

If M_{ai} is independent of T for steady-state transport, the form of Equation 3 makes it clear that L_{ti} increases directly with the cumulative mass of transported sediment, and therefore with both T and flow strength. In contrast, u_{vi} should take a constant mean for steady-state transport conditions and should depend on flow strength, but not T.

Although M_{ai} can be directly measured using the large tracer gravel installations described above, it is useful to define the components of M_{ai} because many tracer observations involve surface grains only and, therefore, may not provide a complete measure of M_{ai}. If entrainment occurs only from the bed surface layer, M_{ai} is given by:

$$M_{ai} = \left(\frac{m_i F_i Y_i}{D_i^2} \right) \tag{5}$$

where the equation is in units of [ML^{-2}], m_i is the mass of a grain of fraction i, F_i is the proportion of fraction i on the bed surface, D_i is fraction size, and Y_i is the proportion of surface grains of fraction i that are entrained over T. The number of grains of size i, per unit bed area, is approximated by F_i/D_i^2, so their mass per unit bed area is $m_i F_i/D_i^2$. Equation 5 is likely to underestimate fractional entrainment at flows larger than those causing full

surface mobilization (Y_i=1) of a fraction. In this case, subsurface grains of that size will also be entrained and M_{ai} becomes proportional to the exchange depth d_x. For Y_i=1·0, M_{ai} becomes:

$$M_{ai} = \left(\frac{m_i F_i}{D_i^3} \right) d_x \tag{6}$$

and the term in parentheses represents the mass of fraction *i* per unit volume which, when multiplied by the exchange depth d_x, gives the mass of fraction *i* entrained per unit bed area.

A smooth transition between the expressions for M_{ai} at partial transport (Equation 5) and fully mobilized transport (Equation 6) may be obtained if it is assumed that $d_x \approx D_i$ for some intermediate value of Y_i. A plausible model takes the exchange depth for a given flow to be equal to the grain size of the fraction for which half of the surface grains are entrained (Y_i=0·5) at that flow. In order that d_x increase consistently with flow strength, it is necessary that the size for which Y_i=0·5 also increase with flow strength, which has been demonstrated for a poorly sorted laboratory sediment (Wilcock and McArdell, 1997). With these assumptions, M_{ai} is given over the full range of transport as:

$$M_{ai} = \left(\frac{m_i F_i Y_i}{D_i^2} \right) \Delta_i \tag{7}$$

with

$$\Delta_i = \begin{cases} 1 & Y_i \le 0 \cdot 5 \\ d_x / D_i & 0 \cdot 5 < Y_i \le 1 \cdot 0 \end{cases} \tag{8}$$

VARIATION OF DISPLACEMENT LENGTH WITH GRAIN SIZE

Basic relations

The relations between the transport components can be used to gain some insight into their functional dependence. We focus here on the variation of L_{ti} with D_i, for which a summary relation of field data is available for comparison (Church and Hassan, 1992). Comparison of Equations 3 and 4 shows that L_{ti} and u_{vi} differ by only a factor of *T*, so many of the conclusions drawn regarding L_{ti} should also apply to u_{vi}. Comparison of the two parts of Equation 8 suggests that the variation of L_{ti} with D_i should be considered separately for partial transport (Y_i<1·0) and fully mobilized transport (Y_i=1·0). For Y_i=1·0, M_{ai} is given by Equation 6. Using the spherical approximation $m_i \approx (\pi/6)\rho_s D_i^3$, Equation 3 becomes:

$$L_{ti} = \frac{q_{bi} T}{(\pi/6)\rho_s F_i d_x} \tag{9}$$

Because d_x is a constant for a given flow, the only terms in Equation 9 that vary with D_i are q_{bi} and F_i. It has been observed that the scaled fractional transport rate q_{bi}/F_i is independent of grain size for sizes smaller than a threshold (e.g. Wilcock, 1992; Wathen *et al*., 1995) that increases with flow strength (Wilcock and McArdell, 1993). Size independence in q_{bi}/F_i occurs when the fractional proportion in transport p_i becomes equal to its proportion in the bed f_i, the condition of equal mobility (Parker *et al*., 1982). Because $q_{bi} = p_i q_b$, where q_b is the total transport rate, q_{bi}/F_i takes the constant value of q_b for all fractions with $p_i/f_i \approx 1$. The relation is approximate because p_i/f_i for equally mobile fractions actually exceeds one as long as p_i/f_i is less than one for any coarser fractions. The onset of equal mobility is closely associated with complete surface mobilization, occurring within one order of magnitude of transport rate of Y_i=1 (Wilcock and McArdell, 1997). For the equally mobile fractions within a mixture, q_{bi}/F_i, and, therefore, L_{ti} should be independent of grain size.

For partial transport conditions, M_{ai} is given by Equations 7 and 8. Considering the case for $Y_i < 0{\cdot}5$, M_{ai} is given by Equation 5, so that Equation 3 becomes:

$$\bar{L}_{ti} = \frac{q_{bi}T}{(\pi/6)\rho_s F_i D_i Y_i} \tag{10}$$

For fractions in a state of partial transport, q_{bi}/F_i decreases rapidly with D_i (Wilcock and McArdell, 1993, 1997), so the effect of both q_{bi}/F_i and D_i in Equation 10 is to cause L_{ti} to decrease rapidly with grain size. Because Y_i also decreases with D_i, the decrease of L_{ti} with D_i is partially balanced by the appearance of Y_i in the denominator of Equation 10, although we will demonstrate below that the decrease of q_{bi} with D_i is more rapid than that of M_{ai}, so that, from Equation 3, L_{ti} decreases with D_i

Based only on the elementary relations for L_{ti} for fully mobilized transport and partial transport and on the fractional transport rates characteristic of these transport regimes, it may be concluded that L_{ti} should be independent of D_i for fully mobilized fractions and should vary inversely with D_i for fractions in a state of partial transport. Before Equations 9 and 10 can be compared with field data, it is necessary to give careful consideration to the manner in which these data are collected and analysed. Two important issues arise. The first concerns the measurement of L_{ti} using tracers placed initially on the bed surface only, so that no subsurface entrainment is measured. The second concerns the choice of using both mobile and immobile grains or mobile grains only when calculating L_{ti}.

For fully mobile fractions, the displacement length determined using only surface tracers should be larger than that calculated by Equation 9, because the total displacement length of surface grains should be greater than the total displacement length for grains originating from both the surface and subsurface (Hassan and Church, 1992). For fully mobilized fractions, the relation between transport rate and the displacement of surface grains is found by setting $\Delta_i = 1$ in Equation 7, so that Equation 3 becomes:

$$\bar{(L_{ti})}_s = \frac{(q_{bi})_s T}{(\pi/6)\rho_s F_i D_i} \tag{11}$$

where (L_{ti})s and $(q_{bi})_s$ are the displacement length and transport rate for surface grains only. For fully mobilized fractions, the total transport rate q_{bi} will include grains that originated from both the surface and subsurface, so that $(q_{bi})_s < q_{bi}$. The relative magnitude of (L_{ti})s may be determined by examining the ratio of Equation 11 and Equation 9:

$$\frac{\bar{(L_{ti})}_s}{\bar{L}_{ti}} = \left(\frac{d_x}{D_i}\right)\left(\frac{(q_{bi})_s}{q_{bi}}\right) \tag{12}$$

For $(q_{bi})_s < q_{bi}$, Equation 12 may be written as:

$$\bar{(L_{ti})}_s < \left(\frac{d_x}{D_i}\right) L_{ti} \tag{13}$$

Equation 13 may then be combined with Equation 9 to define bounds for $(L_{ti})_s$:

$$\frac{q_{bi}T}{(\pi/6)\rho_s F_i d_x} < \bar{(L_{ti})}_s < \frac{q_{bi}T}{(\pi/6)\rho_s F_i D_i} \tag{14}$$

Although the exact relation between $(L_{ti})_s$ and L_{ti} is unspecified, it is seen that $(L_{ti})_s$ is inversely proportional to D_i and larger than L_{ti} by a factor between one and d_x/D_i. For partially mobile fractions, there is likely to be little

or no subsurface entrainment, so $(L_{ti})_s \approx L_{ti}$ and $(q_{bi})_s \approx q_{bi}$ and, to a first approximation, the same result should be obtained regardless of the use of subsurface tracers.

The second necessary consideration when evaluating field measurements of L_{ti} concerns the inclusion of immobile grains in the calculation of L_{ti}, which is important for all fractions with $Y_i < 1$. The value of displacement length calculated using both mobile and immobile grains, $(L_{ti})_{all}$, will be smaller than the value calculated using only mobile grains and is given by:

$$(L_{ti})_{all} = Y_i L_{ti} \tag{15}$$

The inferences drawn regarding the variation of L_{ti} with D_i may be summarized as follows. For grains in a state of equally mobile transport, L_{ti} is independent of D_i and scales with the exchange depth. For grains in a state of partial transport, L_{ti} decreases rapidly with grain size if q_{bi}/F_i decreases more rapidly with D_i than M_{ai}. For fully mobilized fractions, the observed L_{ti} will be greater than that given by Equation 9 by a factor of between 1 and d_x/D_i if L_{ti} is calculated using only surface tracers. For partially mobile fractions, the observed L_{ti} will be smaller than that given by Equation 10 by a factor of Y_i if L_{ti} is calculated using both mobile and immobile tracers.

Calculation of L_{ti} *from transport and entrainment observations*

The total displacement length may be calculated from Equation 3 using measurements of fractional transport rate and bed entrainment. We have measured these quantities in a laboratory experiment (Wilcock and McArdell, 1997), thereby providing the opportunity to illustrate the variation of L_{ti} with D_i in a fashion that, while indirect, makes use of higher quality observations than are often achievable in the field. The laboratory observations include direct observation of partial transport, so that the effect on L_{ti} of the degree of mobilization may be demonstrated, supporting the physical interpretation of L_{ti} developed above.

Recirculating flume experiments were conducted with a widely sorted sediment with $D_{50} = 5{\cdot}3$ mm, a size distribution extending from 0·21 mm to 64 mm, one-third finer than 2·0 mm, and a median size of the portion greater than 2·0 mm equal to 13·5 mm (Wilcock and McArdell, 1993). The sediment was split into 14 size fractions, each of which was painted a different colour to permit measurement of the surface size distribution from point counts on photographs of the bed. The coloured sediment also facilitated the observation of the proportion of each grain size remaining immobile over the duration of the flume runs (Wilcock and McArdell, 1997). The results of four flume runs are used here. Mean bed shear stress varied between 2·0 Pa and 7·3 Pa; the total transport rate varied between 7·5 g ms^{-1} and 572 g ms^{-1}. Detail on the sediment, experimental methods, and surface size distribution measurements may be found in Wilcock and McArdell (1993).

The mobile proportion Y_i of surface grains of all sizes larger than 4·0 mm was measured on time series of bed photographs by noting the presence or absence of individual clasts on the bed surface. An initial set of surface grains of each size was recorded by making drawings of individual grains on projections of photographs taken shortly after the beginning of each run. For fractions in a state of partial transport, the mobile porportion was found to increase rapidly over an initial period and then asymptotically approach a limiting value that varied little with additional run duration. These asymptotic values were used to represent the mobile proportion Y_i of each fraction. Further detail on the entrainment measurements, the time-dependence of surface mobility, and the variation of Y_i with flow strength and grain size (which demonstrate the nature and domain of partial transport) may be found in Wilcock and McArdell (1997)

The variation of Y_i with grain size and flow strength is given in Figure 2a. Partial transport is seen to occur over a range in grain size of approximately a factor of four; the boundaries of the size range increase with flow strength. The corresponding values of Δ_i are calculated from Equation 8 and shown in Figure 2b. Exchange depth d_x is approximated as the size of the fraction observed to be 50 per cent mobile, whose variation with τ_0 can be represented by the power relation (Wilcock and McArdell, 1997):

$$\frac{d_x}{D_{50}} = 397(\tau^*_{50})^{1{\cdot}5} \tag{16}$$

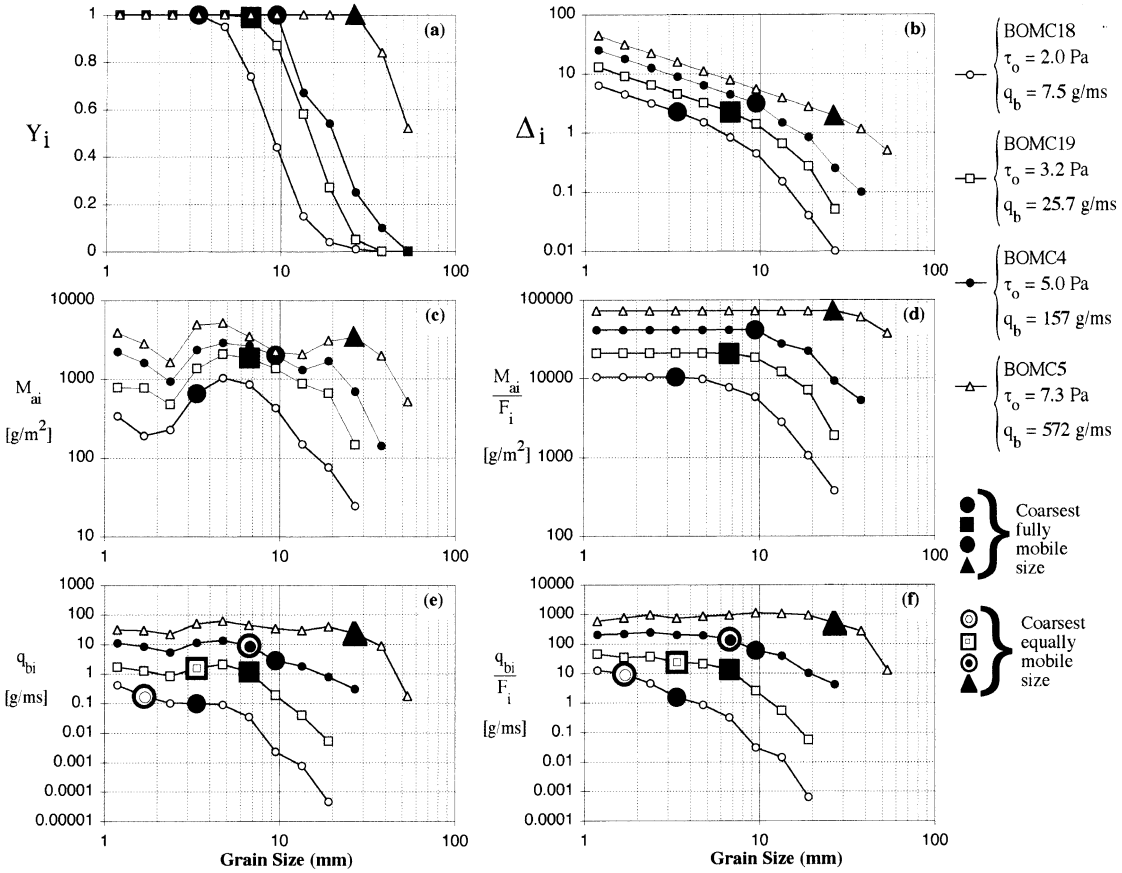

Figure 2. Entrainment and transport observations as a function of grain size from four flume runs with the BOMC sediment. (a) Proportion Y_i of the surface mobilized over the duration of each run. (b) Value of Δ_i calculated from Equation 8 using observed Y_i and d_x estimated from Equation 16. (c) Entrainment per unit bed area calculated from Equation 7 using values of Δ_i in (b). (d) Entrainment per unit bed area scaled with the proportion of each fraction on the bed surface F_i. (e) Fractional transport rates. (f) Fractional transport rates scaled with F_i. Partial transport (y_i<1) occurs over a finite range of sizes of approximately a factor of four; this size range increases with flow strength. Partial transport is associated with rapid decrease with grain size in both entrainment and fractional transport rate

where τ_{50}* is the dimensionless shear stress formed using D_{50} of the sediment mix. M_{ai} is calculated using Equation 7 with measured values of F_i and values of Δ_i from Figure 2b. The measured fractional transport rates are given in Figure 2e. M_{ai} and q_{bi} are scaled by f_i in Figures 2d and 2f. The scaled versions of M_{ai} and q_{bi} are useful because they directly show the variation with D_i of M_{ai} and q_{bi} by eliminating the influence of the proportion of each fraction on the bed surface.

For each run, the largest fully mobile grain (Y_i=1; Figure 2a) is shown by a large grey symbol. The largest equally mobile fraction (operationally defined as $p_i \geq 0{\cdot}9F_i$) is marked on Figures 2e and 2f, which clearly show the association of partial transport, fractional equal mobility, and the size-dependent decrease in transport rate. Fully mobile and equally mobile transport occur at similar values of transport rate. Note that eight orders of magnitude are plotted on the transport axis in Figures 2e and 2f. The decrease of q_{bi} with D_i is more rapid than that of M_{ai} (Figures 2c and 2d), showing that L_{ti} will also decrease with D_i, according to Equation 3.

L_{ti} is calculated using Equations 7, 8 and 16 in Equation 3, along with measured values of q_{bi}, T, τ_0 and Y_i. As suggested by Equations 9 and 10, L_{ti} is independent of D_i for equally mobile fractions and decreases rapidly with D_i for fractions in a state of partial transport (Figure 3). This is particularly clear in Figure 3b, where D_i is scaled by the size of the largest equally mobile fraction D_{em} and L_{ti} is scaled by L_{ti} for that fraction. Recalling that

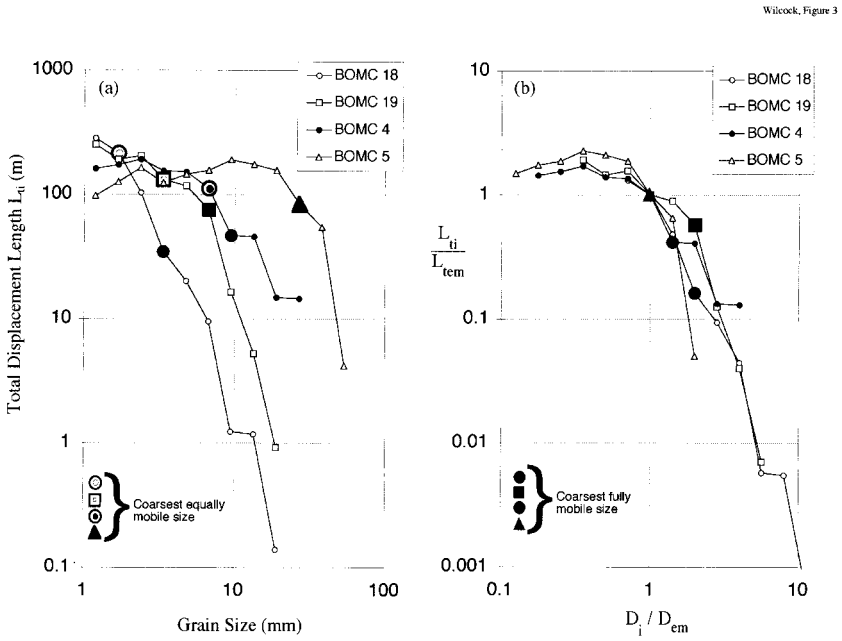

Figure 3. Total displacement length L_{ti} calculated using Equation 3 with values of M_{ai} from Figure 2c and q_{bi} from Figure 2e. (a) L_{ti} as a function of grain size. (b) L_{ti}, scaled by the displacement length of the largest equally mobile fraction, as a function of grain size scaled by the size of the largest equally mobile fraction. The scaled displacement lengths show that L_{ti} is independent of D_i for fully mobile fractions and decreases rapidly with D_i for partially mobile fractions

$L_{ti}=N_iL_{1i}$, the decrease of L_{ti} with D_i can be attributed to an even more rapid decrease of N_i with D_i, because L_{li} has been suggested to be directly proportional to D_i (Nakagawa *et al*., 1982; Drake *et al*., 1988).

Comparison with field data

Church and Hassan (1992) have developed a summary relation for the variation of L_{ti} with D_i using the best available field tracer gravel data. To account for differences in transport rate and flow duration, L_{ti} was scaled using the displacement length of the fraction containing the median size of the bed surface. To account for differences in bed material size distribution, D_i was scaled using the median size of the bed subsurface.

Values of L_{ti} calculated from the laboratory experiment are compared in Figure 4 with the summary relation of Church and Hassan (1992). In Figure 4a, grain size has been scaled using D_{50} of the bulk mix (5·3 mm), which should be similar to the subsurface D_{50} used for the field data. Fractional displacement lengths have been scaled using the displacement length L_{tg} for D_i=13·5 mm, which is the median size of the gravel portion of the mix (D_i >2 mm), which was chosen to approximate the field case for which surface D_{50} was 1·5 to 3·0 times the subsurface D_{50}.

For the two largest transport rates, the scaled displacement lengths calculated for the BOMC runs fall within or near the trend of the field data (Figure 4a). The largest fully mobile grain for these two runs falls near the break in slope of the field relation, suggesting that the decrease in scaled displacement length observed for field data with $D_i/D_{50}>2$ may be associated with partial transport. Scaled L_{ti} for the two runs with smaller transport rates do not follow the field trend, but are displaced towards larger displacement lengths and smaller grain sizes. This is the immediate result of very small calculated displacement lengths for the 13·5 mm fraction for these two runs. Values of Y_i for the 13·5 mm fraction are 0·15 and 0·58 for these two runs, demonstrating that at least one-third of the gravel clasts exposed on the bed surface remained immobile over the duration of the run. This further suggests that the field data may represent cases for which at least the finer half of the bed surface is completely mobilized. If data from smaller transport rates were included in the field compilation, so that partial transport extended to the median and finer fractions, the scaled displacement length for the smaller sizes might

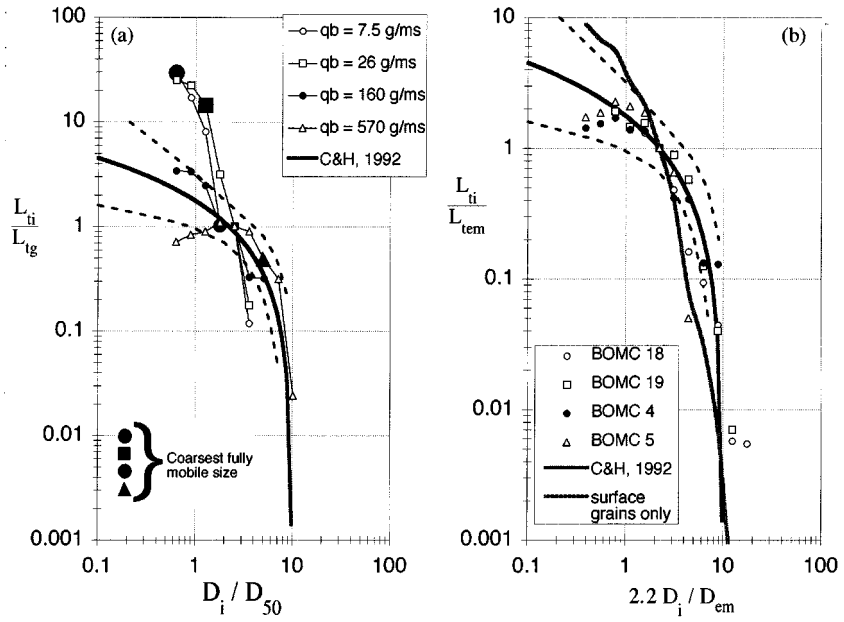

Figure 4. Scaled total displacement length as a function of scaled grain size. Relation of Church and Hassan (1992) for field observations is shown as the solid line; dashed lines are their estimate of 95 per cent confidence error bars for the the relation. (a) L_{ti} scaled by the displacement length of the fraction containing the mean of the gravel portion of the bed; D_i scaled by the median size of the entire sediment mix. (b) L_{ti} scaled by the displacement length of the largest equally mobile fraction; D_i scaled by the size of the largest equally mobile fraction and multiplied by 2·2 to account for the fact that the Church and Hassan relation takes a value of one at a scaled grain size of 2·2. The grey curve in (b) bounds the data trend that would be obtained if the laboratory displacement lengths were measured using only surface tracers and all tracers, mobile and immobile, were included. The scaled displacement lengths calculated from the laboratory observations fall closely about the field trend. This coincidence, the choice of scaling, the arguments associated with Equations (9) and (10), and the direct observation of partial transport in the laboratory case, all suggest that the field relation represents fully mobilized transport for smaller grain sizes and partial transport for larger grain sizes

be expected to be larger than the given trend and to decrease more rapidly with grain size. Both of these factors would produce considerably more scatter in the compilation of field displacement data.

The relation between partial transport and the field trend is more evident in Figure 4b, for which the laboratory data are scaled as in Figure 3b. In Figure 4b, the size ratio is multiplied by 2·2 to make the laboratory case consistent with the field relation, for which the scaled displacement length takes a value of one at $D_i/D_{50} = 2{\cdot}2$. Also shown in Figure 4b is the trend for L_{ti} that would result for the laboratory data if only surface tracers were used and if both immobile and mobile grains were used to calculate L_{ti}, as done by Church and Hassan (1992). Although Equations 14 and 15 produce a different relation for each run, the curves are very similar in the scaled domain of Figure 4b, so only a single mean relation is shown. For $D_i < D_{em}$, the true surface-only relation for the laboratory data should fall between the plotted data and the surface-only curve. The laboratory data follow the field trend closely for all sizes and runs. The similarity in shape of the field curve and the laboratory data, together with the direct observation of partial transport and the relative location of the largest fully mobile fraction on each curve, suggest that the field summary of displacement lengths represents fully mobilized transport for finer fractions and partial transport for coarser fractions.

DISCUSSION

The spatial variability of bed composition, flow and transport in natural streams requires that comparison between the laboratory data and field relation in Figure 4b be made carefully. The laboratory data are for an essentially uniform transport field. In the field, local entrainment may vary widely and the observed displacement lengths can represent a combination of fully mobilized and partial transport in different locations. Although this could be considered to be partial transport in a spatially averaged sense, important differences can arise relative to the uniform transport case.

Consider the extreme but simple example in which the coarsest fraction D_{max} in the central one-half of the bed is almost completely mobilized, whereas the remaining half of the bed along the channel margins is completely immobile. In this case, the spatially averaged mobilized proportion is 0·5 for all fractions. According to Equation 5, M_{ai} for each fraction would be given by $[0{\cdot}5(\pi/6)\rho_s F_i D_i]$. When combined with observed values of L_{ti}, this value of M_{ai} would underestimate the transport rate of all fractions except the largest, because the subsurface mobilization of the finer fractions in the central portion of the channel has not been accounted for. Entrainment in the central portion of the channel is actually given by Equation 6 as $[(\pi/6)\rho_s F_i d_x]$ with d_x approximately equal to D_{max}. When reduced by half to account for the immobile portion of the channel, the spatial average of M_{ai} is $[0{\cdot}5(\pi/6)\rho_s F_i D_{max}]$, showing that the underestimate of M_{ai} made by using $Y_i = 0{\cdot}5$ is given by D_i/d_x. To accurately calculate M_{ai} and fractional transport rates, it is necessary to know the spatial distribution of Y_i and d_x and calculate the total transport rate as the spatial integral of the local transport rate.

Calculation of transport from entrainment and displacement observations reflects a spatial average over the distance of displacement. In contrast, calculation of displacement lengths from entrainment and transport observations gives a *local* measure of displacement at the location of the entrainment and transport measurements. Any spatial variation in transport rate will have a corresponding variation in entrainment and displacement length, so that the actual displacement lengths will differ from their local estimate if the transport field is spatially variable.

The influence of grain shape was not systematically measured in the BOMC laboratory work, nor is it accounted for in the summary relation of Church and Hassan (1992). In a study of 480 magnetic-core tracers during two moderate flood events on a step-pool channel, Schmidt and Ergenzinger (1992) observed similar displacement frequencies and distances for tracer grains of rod, ellipsoid and spherical shape, but found that the entrainment frequency of discs was as little as half and the mean displacement length was a factor of three smaller than the other shape classes. The BOMC grains fall within the sphere and ellipsoid classes reported by Schmidt and Ergenzinger, and shape information is not available for all of the data summarized by Church and Hassan. Most of the scatter in their summary plot falls within a factor of three; uncontrolled variation in grain shape is one of several likely causes of this scatter.

CONCLUSIONS

Tracer gravels may be installed in a gravel bed by inserting a large cylinder into the bed and replacing the sediment within with marked grains of the same size distribution. The mass difference of tracers before and after a flow event gives a direct measure of the entrainment per area for each size, which may be directly used in calculations of sediment transport rate. The tracers also provide a local measure of the proportion and size distribution of mobilized sediment, giving information on the size-selective exchange of sediment between flow, bed surface and subsurface, which is needed to understand bed armouring, selective deposition and subsurface flushing. Installation of tracers below the depth of scour eliminates uncertainties associated with estimating entrainment from surface tracers alone. The labour involved in replacing a section of bed with tracer gravels is considerable, although partly offset by the fact that size distributions of the surface and subsurface are obtained in the process. Large tracer gravel installations may be used in combination with scour chains or other scour depth indicators to provide more measurements and broader coverage along with an estimate of the mass and size distribution of entrained sediment.

Calculation of transport rate from tracer gravel observations requires an explicit statement of the relation between transport rate, entrainment and displacement length. The relation also provides a basis for evaluating tracer data collected by different methods. When calculating transport rates, particular attention must be given to whether the tracers are placed only on the bed surface, or in both the surface and subsurface, and to whether both mobile and immobile tracers are included in the calculations. Total displacement length depends on the cumulative product of transport rate and flow duration, so that both flow strength and sediment properties are important, as indicated by any transport rate relation.

The formal relation between transport, entrainment and displacement may be used to provide physical insight regarding the expected behaviour of tracer grains. The variation of displacement length with grain size depends on the degree of mobilization of the individual fractions in the bed. For finer fractions in a state of

equally mobile transport (in which the proportion in transport equals or exceeds that in the bed), total displacement length may be expected to be independent of grain size. For coarser fractions in a state of partial transport (in which a portion of the surface grains remains immobile throughout the flow event), total displacement length should decrease rapidly with grain size. These relations are supported by displacement lengths calculated from observed entrainment and transport rate in a laboratory flume. Comparison of these results with a summary relation for field displacement data suggests that the field relation represents flow and transport conditions for which the finer fractions are fully mobilized, whereas the coarser fractions are in a state of partial transport.

ACKNOWLEDGEMENTS

Fieldwork on the Trinity River was supported by US Fish and Wildlife Service, Trinity River Flow Study. The laboratory experiments were supported by grant N00014–19-J-1192 from the US Office of Naval Research and grant EAR–9004206 from the US National Science Foundation. The subsequent analysis of grain immobility was supported by grant EAR–9205511 from the US National Science Foundation. The paper benefited considerably from discussions and review of an earlier draft by Judy Haschenburger, and from review comments by Marwan Hassan and Peter Ergenzinger.

REFERENCES

Church, M. and Hassan, M. A. 1992. 'Size and distance of travel of unconstrained clasts on a streambed', *Water Resour. Res.*, **28**, 299–303.

Church, M. A., McLean, D. G. and Wolcott, J. F. 1987. 'River bed gravels: sampling and analysis', in Thorne, C. R., Bathurst, J. C. and Hey, R. D. (Eds), *Sediment Transport in Gravel-bed Rivers*, John Wiley & Sons, Chichester.

Drake, T. G., Shreve, R. L., Dietrich, W. E., Whiting, P. J. and Leopold, L. B. 1988. 'Bedload transport of fine gravel observed by motion-picture photography', *J. Fluid Mech.*, **192**, 193–217.

Einstein, H. A. 1937. *Bedload transport as a probability problem*, PhD thesis, translated by W. W. Sayre, in Shen, H- W. (Ed.), 1972. *Sedimentation*, Colorado State University App. C.

Emmett, W. W., Burrows, R. L. and Chacho, E., F. Jr. 1990. 'Coarse particle transport in a gravel-bed river', paper presented at *International Workshop on Gravel-Bed Rivers: Dynamics of Gravel-Bed Rivers*, Florence, Italy, September 1990.

Ergenzinger, P. and Conrady, J. 1982. 'A new tracer technique for measuring bedload in natural channels', *Catena*, **9**, 77–80.

Fernandez Luque, R. and Van Beek, R. 1976. 'Erosion and transport of bedload sediment', *J. Hydraul. Res.*, **14**(2), 127–144.

Haschenburger, J. K. 1996. *Scour and fill in a gravel-bed channel: observations and stochastic models*, PhD thesis, University of British Columbia, 144 pp.

Hassan, M. A. and Church, M. 1992. 'The movement of individual grains on the streambed', in Billi, P., Hey, R. D., Thorne, C. R. and Tacconi, P. (Eds), *Dynamics of Gravel-bed Rivers*, John Wiley & Sons, Chichester.

Hassan, M. A. and Church, M. 1994. 'Vertical mixing of coarse particles in gravel bed rivers: a kinematic model', *Water. Resour. Res.*, **30**, 1173–1185.

Hassan, M. A., Church M. and Ashworth, P. J. 1992. 'Virtual rate and mean distance of travel of individual clasts in gravel-bed channels', *Earth Surf. Processes Land.*, **17**, 617–627.

Hassan, M. A., Church, M. and Schick, A. P. 1991. 'Distance of movement of coarse particles in gravel-bed streams'.

Hassan, M. A., Schick, A. P. and Laronne, J. B. 1984. 'The recovery of flood-dispersed coarse sediment particles', *Catena Suppl.* **5**, 153–162.

Kirkby, M. J. 1991. 'Sediment travel distance as an experimental and model variable in particulate movement', *Catena Suppl.* **19**, 111–128.

McNeil, W. and Ahnell, W. 1964. *Success of pink salmon spawning relative to size of spawning bed materials*, US Fish and Wildlife Service Special Scientific Report, Fisheries **469**.

Nakagawa, H., Tsujimoto, T. and Nakano, S. 1982. 'Characteristics of sediment motion for respective grain sizes of sand mixtures', *Bulletin, Disaster Prevention Research Institute, Kyoto Univ.*, **32**(1), 1–32.

Parker, G., Klingeman, P. C. and McLean, D. L. 1982. 'Bedload and size distribution in paved gravel-bed streams', *J. Hydraul. Div. ASCE*, **108**(HY4), 544–571.

Rood, K. and Church, M. 1994. 'Modified freeze-core technique for sampling the permanently wetted streambed', *N. Am. J. Fisheries Manage.* **14**, 852–861.

Schick, A. P., Hassan, M. A. and Lekach, J. 1987. 'A vertical exchange model for coarse bedload movement: numerical considerations', *Catena Suppl.* **10**, 73–83.

Schmidt, K-. H. and Ergenzinger, P. 1992. 'Bedload entrainment, travel lengths, step lengths, rest periods – studied with passive (iron, magnetic) and active (radio) tracer techniques', *Earth Surf. Processes Land.*, **17**, 147–165.

Stelczer, K. 1981. *Bedload Transport: Theory and Practice*, Water Resources Publications, Littleton CO, 295 pp.

Wathen, S. J., Ferguson, R. I. Hoey, T. B. and Werrity, A. 1995. 'Unequal mobility of gravel and sand in weakly bimodal river sediments', *Water Resour. Res.*, **31**(8), 2087–2096.

Wilcock, P. R. 1992. 'Experimental investigation of the effect of mixture properties on transport dynamics', in Billi, P., Hey, R. D., Thorne, C. R. and Tacconi, P. (Eds), *Dynamics of Gravel-bed Rivers*, John Wiley & Sons, Chichester, 109–139.

Wilcock, P. R. and McArdell, B. W. 1993. 'Surface-based fractional transport rates: mobilization thresholds and partial transport of a sand-gravel sediment', *Water Resour. Res.*, **29**(4), 1297–1312.
Wilcock, P. R. and McArdell, B. W. 1997. 'Partial transport of a sand-gravel sediment', *Water Resour. Res.*, **33**(1), 233–245.
Wilcock, P. R., Barta, A. F., Shea, C. C., Kondolf, G. M., Matthews, W. V. G. and Pitlick, J. C. 1996. 'Observations of flow and sediment entrainment on a large gravel-bed river', *Water Resour. Res.*, **32**(9), 2897–2909.

